

Hybrid exchange-correlation energy functionals for strongly correlated electrons: Applications to transition-metal monoxides

Fabien Tran, Peter Blaha, and Karlheinz Schwarz

Institute of Materials Chemistry, Vienna University of Technology, Getreidemarkt 9/165-TC, A-1060 Vienna, Austria

Pavel Novák

Institute of Physics, Academy of Sciences of the Czech Republic, Cukrovarnická 10, CZ-162 53 Prague 6, Czech Republic

(Received 9 May 2006; revised manuscript received 23 August 2006; published 12 October 2006)

For the treatment of strongly correlated electrons, the corresponding Hartree-Fock exchange energy is used instead of the local density approximation (LDA) or generalized gradient approximation (GGA) functional, as suggested recently [P. Novák *et al.*, Phys. Status Solidi B **243**, 563 (2006)]. If this is done only inside the atomic spheres, using an augmented plane wave scheme, a significant simplification and reduction of computational cost is achieved with respect to the usual but costly implementation of the Hartree-Fock formalism in solids. Starting from this, we construct exchange-correlation energy functionals of the hybrid form like B3PW91, PBE0, etc. These functionals are tested on the transition-metal monoxides MnO, FeO, CoO, and NiO, and the results are compared with the LDA, GGA, LDA+ U , and experimental ones. The results show that the proposed method, which does not contain any system-dependent input parameter, gives results comparable or superior to the ones obtained with LDA+ U which is designed to improve significantly over the LDA and GGA results for systems containing strongly correlated electrons. The computational efficiency, similar to the LDA+ U one, and accuracy of the proposed method show that it represents a very good alternative to LDA+ U .

DOI: [10.1103/PhysRevB.74.155108](https://doi.org/10.1103/PhysRevB.74.155108)

PACS number(s): 71.15.Mb, 71.15.Ap, 71.27.+a, 71.20.Be

I. INTRODUCTION

Nowadays, the Kohn-Sham¹ version of density functional theory² is the most widely used quantum mechanical method to calculate the electronic properties of molecules and solids. Since the mid-1990s, the most successful approximate functionals for the exchange-correlation energy for molecules are the hybrid methods,^{3,4} which, e.g., have an accuracy of 2–3 kcal/mol for the binding energy of covalent bonds.⁵ The hybrid functionals constitute the state-of-the-art in quantum chemistry since they are able to provide reliable results in a lot of circumstances at a cost which is only slightly higher than a calculation using the local density approximation (LDA) or the generalized gradient approximation (GGA). For solids, the LDA and GGA approximations are still extensively used, giving satisfying results for most applications. Although LDA and GGA are still very successful approximations for solids, there are some problems for which better functionals for the exchange-correlation energy are needed. Despite some earlier implementations of the Hartree-Fock (HF) method (needed to apply hybrid functionals) for solids (see, e.g., Refs. 6–9), it is only since about 2000 that calculations on solids with hybrid functionals began to appear (see, e.g., Refs. 10 and 11). One of the reasons was the technical difficulty to efficiently apply HF exchange to solids. Since then some of these difficulties have been overcome and different implementations of HF^{12–18} or Kohn-Sham exact exchange (i.e., HF energy expression with a local multiplicative potential)^{19–21} have been reported for solid-state calculations. Now, more and more solid-state calculations are being performed with hybrid functionals (see Ref. 22 for a recent review), but these calculations are still far from being applied routinely due to the high computa-

tional cost which is required when using the HF exchange.

One among the problems of LDA and GGA calculations mentioned above is the band gap problem; when the Kohn-Sham eigenvalues are used for estimating excitation energies, which rigorously should not be done but often is, the calculated band gaps of insulators or semiconductors are systematically too small (or even absent) relative to the experimental values. Another well-known problem is the incorrect description of localized (strongly correlated) d and f electrons in transition-metal and rare-earth compounds, respectively. Mainly responsible for these deficiencies is the self-interaction error (SIE) contained in LDA and GGA functionals. As hybrid functionals contain a fraction of HF exchange, which does not have any SIE, they greatly improve (with respect to LDA and GGA) the calculation of band gaps and the description of localized d and f electrons.

Recently, Novák *et al.*¹⁸ proposed an improvement of the description of strongly correlated electrons by subtracting the LDA or GGA exchange-energy functional corresponding to the subspace of the states of the correlated electrons and to add the HF expression instead. This method, called “exact exchange for correlated electrons,” was implemented within the full-potential (linearized) augmented plane-wave plus local orbitals [FP-(L)APW+lo] method and it was successfully applied to several $3d$ and $4f$ systems. In this work we present results of this scheme including hybrid functionals. In order to illustrate the performance of the method, we choose compounds with strongly correlated d electrons, namely MnO, FeO, CoO, and NiO.

The paper is organized as follows. In Sec. II, the outline of the method and the computational details are given. In Sec. III, the results are presented and discussed, and in Sec. IV a summary and conclusion is given.

II. METHOD AND COMPUTATIONAL DETAILS

In the present scheme, three hybrid functionals are applied but only to a selected set of electrons, namely the ones that are poorly treated by LDA and GGA.

At first we chose the PBE0^{23,24} hybrid functional, for which the exchange-correlation energy is

$$E_{xc}^{\text{PBE0}}[\rho] = E_{xc}^{\text{PBE}}[\rho] + \frac{1}{4}(E_x^{\text{HF}}[\Psi_{\text{sel}}] - E_x^{\text{PBE}}[\rho_{\text{sel}}]), \quad (1)$$

where Ψ_{sel} and ρ_{sel} represent the wave function and the corresponding electron density of the selected (sel) electrons, respectively. From Eq. (1), we can see that the GGA PBE (Ref. 25) exchange-correlation energy functional is derived from the total electron density, and a fraction of HF exchange replaces the GGA PBE exchange but only for the selected electrons. In Eq. (1), the fraction 1/4 of HF exchange was determined from fourth order perturbation theory considerations.²⁶

The second hybrid functional is the one proposed by Becke,⁴

$$\begin{aligned} E_{xc}^{\text{B3PW91}}[\rho] &= E_{xc}^{\text{LDA}}[\rho] + 0.2(E_x^{\text{HF}}[\Psi_{\text{sel}}] - E_x^{\text{LDA}}[\rho_{\text{sel}}]) \\ &+ 0.72(E_x^{\text{B88}}[\rho] - E_x^{\text{LDA}}[\rho]) \\ &+ 0.81(E_c^{\text{PW91}}[\rho] - E_c^{\text{LDA}}[\rho]), \end{aligned} \quad (2)$$

where $E_x^{\text{LDA}} = E_x^{\text{Dirac}}$,²⁷ $E_c^{\text{LDA}} = E_c^{\text{PW92}}$ is the LDA correlation-energy functional of Perdew and Wang,²⁸ E_x^{B88} is the GGA exchange-energy functional proposed by Becke in 1988,²⁹ and E_c^{PW91} is the GGA correlation part of the Perdew and Wang functional.³⁰ The three parameters in Eq. (2) (0.2, 0.72, and 0.81) were chosen in order to reproduce experimental thermochemical data.⁴

The third hybrid functional considered was proposed by Moreira *et al.*,³¹

$$E_{xc}^{\text{Fock-}\alpha}[\rho] = E_{xc}^{\text{LDA}}[\rho] + \alpha(E_x^{\text{HF}}[\Psi_{\text{sel}}] - E_x^{\text{LDA}}[\rho_{\text{sel}}]), \quad (3)$$

where $E_c^{\text{LDA}} = E_c^{\text{PW92}}$ [Moreira *et al.*³¹ used $E_c^{\text{LDA}} = E_c^{\text{VWN}}$ (Ref. 32)], which is of the same form as Eq. (1), but LDA replacing PBE. Two values for the fraction α of HF exchange will be used: 0.35 and 0.5, giving functionals Fock-0.35 and Fock-0.5, respectively.

The calculation of the HF term E_x^{HF} is done in an approximate way as explained in Ref. 18 and implemented into the WIEN2k code³³ which is based on the FP-(L)APW+lo method. The scheme looks very similar to the LDA+ U method,^{34–36} and here the rotationally invariant version^{35,36} is adopted for the calculation of E_x^{HF} . This term is only used for those electrons that correspond to a certain angular momentum ℓ of a selected atom,

$$E_x^{\text{HF}}[\Psi_{\text{sel}}] = -\frac{1}{2} \sum_{\sigma} \sum_{m_1, m_2, m_3, m_4} n_{m_1, m_2}^{\sigma} n_{m_3, m_4}^{\sigma} \langle m_1 m_3 | v_{ee} | m_4 m_2 \rangle, \quad (4)$$

where n_{m_i, m_j}^{σ} ($m_i = -\ell, \dots, \ell$ and σ is the spin index) is the occupation matrix and $v_{ee} = 1/|\mathbf{r}_1 - \mathbf{r}_2|$ is the unscreened Coulomb operator (in atomic units). The integrals in Eq. (4) are calculated as

$$\langle m_1 m_3 | v_{ee} | m_4 m_2 \rangle = \sum_{k=0}^{2\ell} a_k(m_1, m_3, m_4, m_2) F^k, \quad (5)$$

where

$$\begin{aligned} a_k(m_1, m_3, m_4, m_2) &= \frac{4\pi}{2k+1} \sum_{q=-k}^k \langle Y_{\ell m_1} | Y_{kq} | Y_{\ell m_4} \rangle \\ &\times \langle Y_{\ell m_3} | Y_{kq}^* | Y_{\ell m_2} \rangle \end{aligned} \quad (6)$$

and F^k are the Slater integrals,

$$F^k = \int_0^{R_{MT}} \int_0^{R_{MT}} \chi_{\ell}^2(r_1) \chi_{\ell}^2(r_2) \frac{r_{<}^k}{r_{>}^{k+1}} r_1^2 r_2^2 dr_1 dr_2, \quad (7)$$

where $r_{<} = \min(r_1, r_2)$ and $r_{>} = \max(r_1, r_2)$, and $\chi_{\ell}(r)$ is a radial function whose calculation is explained in Ref. 18. These expressions are evaluated only inside the atomic spheres of the FP-(L)APW+lo method as it is done for LDA+ U .³⁷ In the present work this should not be a problem, since Eqs. (4)–(7) are applied to d electrons which are essentially localized inside the corresponding spheres. The present scheme follows the same strategy as employed for LDA+ U , but there are two major differences. First, the Slater integrals [Eq. (7)] are directly calculated instead of being treated as adjustable parameters as in LDA+ U to reproduce experiment. Second, the removal of the LDA or GGA exchange term for the selected electron density is done by using the correct expression [e.g., $E_x^{\text{PBE}}[\rho_{\text{sel}}]$ for PBE0 in Eq. (1)] and not approximately as in LDA+ U . In the latter case the whole (Coulomb and exchange) double counting (dc) term for the fully localized version is given by

$$E_{\text{dc}} = U \frac{n_{\ell}(n_{\ell} - 1)}{2} - J \sum_{\sigma} \frac{n_{\ell}^{\sigma}(n_{\ell}^{\sigma} - 1)}{2}, \quad (8)$$

where n_{ℓ}^{σ} is the total number of σ electrons for the selected ℓ and $n_{\ell} = n_{\ell}^{\uparrow} + n_{\ell}^{\downarrow}$. These differences make the present method more appealing than LDA+ U since the present scheme does not contain any system-dependent parameters, in contrast to choosing U and J in LDA+ U . Only the amount of HF exchange can be varied, but after selecting a particular functional this quantity is kept fixed. For more details about the method, see Novák *et al.*,¹⁸ and about the calculation of the occupation matrix and the orbital-dependent potential, see Ref. 37 [implementation of LDA+ U within the FP-(L)APW+lo framework].

In order to compare the performance of the present hybrid scheme with the alternative LDA+ U method, we selected the transition-metal monoxides MnO, FeO, CoO, and NiO, which exhibit strong correlation effects among the d electrons. These extensively studied systems are very difficult cases for LDA (Ref. 38) and GGA (Ref. 39) which lead to band gaps and magnetic moments that are too small since both, LDA and GGA, do not sufficiently localize these d electrons. For all four systems, the type-II antiferromagnetic

state (AFII) was studied, which experimentally was found to be the ground state. The structure of the compounds is of the rock-salt type (space group $Fm\bar{3}m$, number 225), but considering the antiferromagnetic order along the [111] direction of the AFII phase, the symmetry is reduced to a rhombohedral one (space group $R\bar{3}m$, number 166). For a schematic representation of the structure see Fig. 6 of Ref. 40. The experimentally observed distortions from the rock-salt structure of these compounds are small and were neglected in our calculations. For comparison LDA, GGA (PBE), and LDA+ U calculations were also performed. For the LDA+ U calculations the values of U and J , as determined by Anisimov *et al.*³⁴ from the constrained-density-functional method, were used with $U_{\text{eff}}=U-J$. The values of U_{eff} are 6.04, 5.91, 6.88, and 7.05 eV for MnO, FeO, CoO, and NiO, respectively.

All our calculations were done with the WIEN2k code³³ which is based on FP-(L)APW+lo method to solve the Kohn-Sham equations. The Brillouin zone integrations were performed with a $17 \times 17 \times 17$ special point grid and $R_{MT}^{\text{min}}K_{\text{max}}=8$ (the product of the smallest of the atomic sphere radii R_{MT} and the plane wave cutoff parameter K_{max}) was used for the expansion of the basis set in order to ensure good convergence of the different calculated quantities. The spheres radii of the transition metal (M) and oxygen atoms (O) were chosen as $(R_{MT}^M, R_{MT}^O)=(2.15, 1.82)$, $(2.1, 1.77)$, $(2.05, 1.75)$, and $(2.0, 1.73)$ a.u. for MnO, FeO, CoO, and NiO, respectively. They were chosen in such a way that for the smallest volume of the unit cell we considered the spheres are nearly touching. For the determination of the lattice constant and bulk modulus these sphere radii were kept constant. According to tests we did, with this choice for the R_{MT} , the spheres of the transition metals are sufficiently large so that the leakage of the d electrons outside the spheres is sufficiently small not to affect the results. For instance, with B3PW91, enlarging R_{MT}^{Mn} from 2.15 to 2.3 a.u. for MnO increases the spin magnetic moment by only $0.08\mu_B$ and the band gap by less than 0.02 eV. The increase of the Mn atom magnetic moment (a quantity for which a unique definition does not exist) is mainly due to the larger region of integration for its determination as the same increase is obtained with the PBE functional. For the other transition metals (whose $3d$ electrons are more localized) smaller changes are observed. A similar test for NiO with $R_{MT}^{\text{Ni}}=2.2$ a.u. leads to essentially unchanged results (increases of $0.002\mu_B$ for the spin magnetic moment and 0.02 eV for the band gap).

The spin magnetic moment M_s , fundamental band gap Δ_{fund} , and optical band gap Δ_{opt} (lowest direct dipole-allowed transition energy) were evaluated at the experimental geometry. For FeO and CoO, spin-orbit coupling effects were included to calculate the orbital magnetic moment M_ℓ which is supposed to be large for these two compounds. The lattice constant a and bulk modulus B were determined from the Birch-Murnaghan equation of state and without the spin-orbit coupling effects. We checked that the inclusion of spin-orbit coupling insignificantly changes these two properties.

TABLE I. Calculated and experimental lattice constant a (Å), bulk modulus B (GPa), spin magnetic moment M_s (μ_B), fundamental band gap Δ_{fund} (eV), and optical band gap Δ_{opt} (eV) of AFII phase of MnO.

	a	B	M_s	Δ_{fund}	Δ_{opt}
LDA	4.32	184	4.19	0.8	1.0
PBE	4.45	147	4.26	0.9	1.4
PBE ^a	4.37		4.31	1.44	
LDA+ U	4.40	174	4.50	1.9	2.5
B3PW91	4.46	154	4.38	1.3	1.9
B3LYP ^b	4.495		4.73	3.92	
PBE0	4.51	143	4.40	1.3	1.9
PBE0 ^a	4.40		4.52	4.02	
Fock-0.35	4.41	174	4.41	1.5	2.1
Fock-0.5	4.44	170	4.46	1.7	2.3
Expt.	4.445 ^c	151 ^d , 162 ^e	4.58 ^f , 4.79 ^g	3.9 ^h	2.0 ⁱ

^aReference 42.

^dReference 45.

^gReference 48.

^bReference 43.

^eReference 46.

^hReference 49.

^cReference 41.

^fReference 47.

ⁱReference 53.

III. RESULTS

A. MnO

From the results presented in Table I, we can see that LDA gives a too small lattice constant of 4.32 Å with respect to the experimental value of 4.445 Å,⁴¹ while PBE yields the very accurate value of 4.45 Å. LDA+ U gives a value (4.40 Å) which is too short by about 0.05 Å. Among the hybrid functionals, B3PW91 and Fock-0.5 are the ones giving the best lattice constants, deviating by less than 0.02 Å from the experimental value. Comparing our version of the PBE0 functional with the conventional version (HF applied to all electrons), we observe the same trend for the lattice constant when going from PBE to PBE0. Franchini *et al.*⁴² reported an increase of the lattice constant of 0.03 Å which is close to our value of 0.06 Å. The value $a=4.495$ Å calculated by Feng⁴³ with B3LYP⁴⁴ (supposed to give similar results as B3PW91) is slightly larger than our B3PW91 value of $a=4.46$ Å. For the bulk modulus B , only the B3PW91 hybrid functional gives a value falling within the experimental range of 151–162 GPa.^{45,46}

As expected (see, e.g., Ref. 39), LDA and GGA give too small values of $\sim 4.2\mu_B$ for the spin magnetic moment M_s in comparison with the available experimental values [4.58 (Ref. 47) and 4.79 (Ref. 48) μ_B]. LDA+ U and hybrid functionals give higher values of M_s , which means a better agreement with experiments. LDA+ U gives the largest value, $4.50\mu_B$, which is slightly larger than the value obtained with the Fock-0.5 hybrid functional ($4.46\mu_B$). Applying the conventional PBE0 hybrid functional, Franchini *et al.*⁴² reported, with respect to PBE, an increase of the spin magnetic moment of $0.21\mu_B$, a trend which is fairly well reproduced by our implementation of the PBE0 functional with an increase of $0.14\mu_B$.

Figure 1 shows the calculated density of states (DOS) of MnO of some selected functionals (LDA, LDA+ U , PBE0,

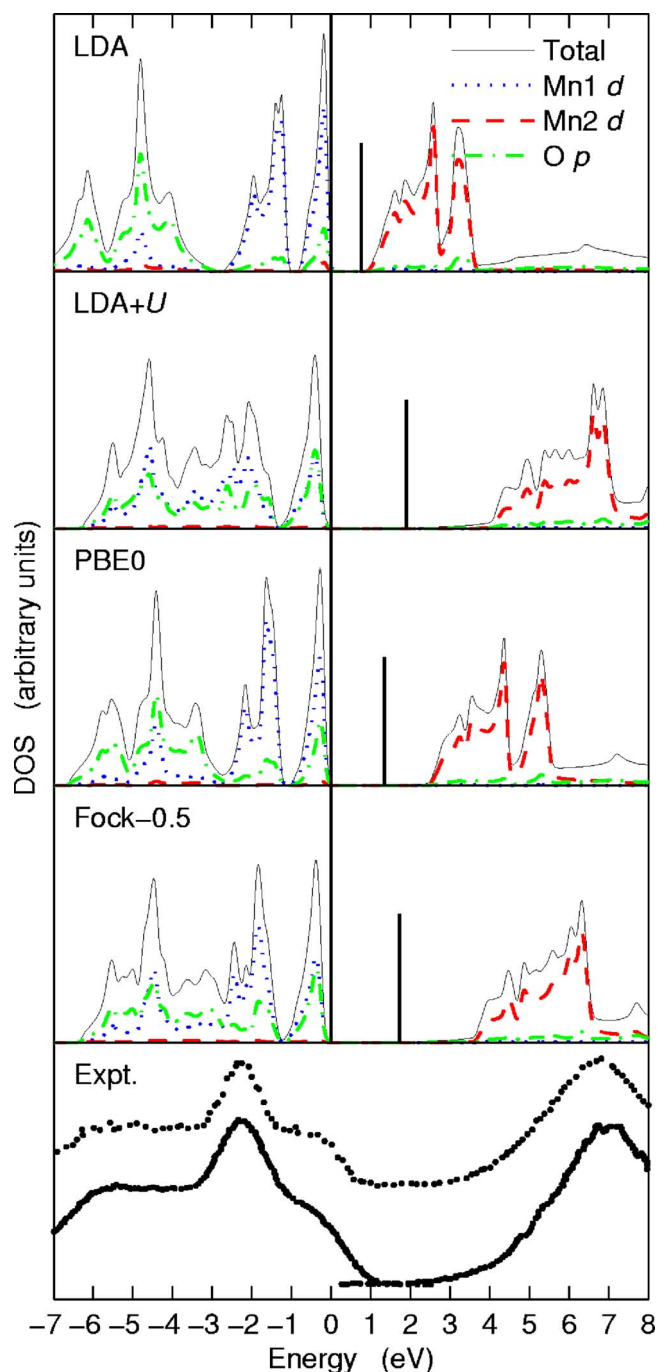


FIG. 1. (Color online) Total and projected calculated DOS of one spin component of AFII phase of MnO. The vertical bars indicate the end of the fundamental band gap which starts at $E=0$ eV (Fermi energy). The lowest panel shows curves obtained from XPS/BIS measurements by van Elp *et al.* (Ref. 49) (lower curve) and Zimmermann *et al.* (Ref. 50) (upper curve).

and Fock-0.5), as well as the x-ray photoemission spectroscopy (XPS) and inverse photoemission spectroscopy [bremsstrahlung-isochromat spectroscopy (BIS)] measurements of van Elp *et al.*⁴⁹ and Zimmermann *et al.*⁵⁰ The horizontal position of the XPS/BIS curves was chosen such that the shoulder in the XPS spectra matches the highest valence band peak of the theoretical DOSs. A similar procedure was

done for the other systems discussed in the next sections. We can see that LDA+ U and hybrid functionals give a band gap which is of mixed Mott-Hubbard/charge-transfer character, i.e., the O 2*p* states contribute significantly to the DOS just below the Fermi energy. This observation is in accordance with experimental reports.^{49,51,52} With LDA+ U and Fock-0.5 the contributions from Mn 3*d* and O 2*p* states are of about 50%. LDA and PBE give a contribution of O 2*p* states which is much smaller. Comparing our calculated DOSs with the XPS/BIS (Refs. 49 and 50) curves, we observe that only LDA+ U (and eventually Fock-0.5) yields a DOS in qualitative agreement with XPS/BIS measurements. With less HF exchange (or a smaller U_{eff}) the *d* peaks of the unoccupied part of the DOS are not sufficiently pushed above the Fermi energy. The band gap of about 3.9 eV determined by van Elp *et al.*⁴⁹ is significantly larger than our calculated values of the fundamental band gap Δ_{fund} (indirect with all functionals) which are situated between 1.3 and 1.9 eV for the orbital-dependent potentials. This disagreement should be considered with care, since the way van Elp *et al.*⁴⁹ determined the band gap is rather approximate. In particular, they chose the end of the band gap at 10% intensity of the rising Mn 3*d* structure, whereas according to our analysis, a significant part of the long tail starting after the fundamental band gap of our calculated DOSs comes from Mn 4*s* electrons. The optical band gap Δ_{opt} was also calculated, and from the results we see that B3PW91, PBE0, and Fock-0.35 hybrid functionals give values which are in very good agreement with the experimental value [2.0 eV (Ref. 53)], while LDA+ U and Fock-0.5 values are slightly larger.

B. FeO

The results for FeO presented in Table II show that LDA underestimates the lattice constant a by about 0.15 Å with respect to the experimental value of 4.334 Å.⁵⁴ PBE and LDA+ U improve over LDA, but still underestimate a by about 0.05 Å. B3PW91 and Fock-0.5 are the best performing functionals with 4.35 and 4.34 Å, respectively. We note that the B3PW91 value is close to the value 4.365 Å calculated by Alfredsson *et al.*⁵⁵ with the conventional implementation of the B3LYP hybrid functional. The values $B=172$ and 155 GPa obtained with B3PW91 and PBE0 hybrid functionals for the bulk modulus are the only ones to fall within the experimental range of 150–180 GPa (see Ref. 56 and references therein).

For the total magnetic moment $M=M_s+M_\ell$, LDA and GGA give values which are situated between the reported experimental values of 3.32 (Ref. 57) and 4.2 (Ref. 58) μ_B . Nevertheless, in Refs. 59 and 60 it is argued that for FeO the orbital magnetic moment M_ℓ could have a value of about 1 μ_B and the total experimental value of 4.2 μ_B (Ref. 58) should be more likely. Therefore, the results obtained with LDA+ U and hybrid functionals, that give values of 0.6–0.75 μ_B for M_ℓ , can be considered as very good.

From the DOSs shown in Fig. 2, we can see that using an orbital-dependent potential for the *d* electrons (LDA+ U or hybrid) splits the metallic LDA or PBE DOS around the Fermi energy (essentially of Fe 3*d* character) into two well

TABLE II. Calculated and experimental lattice constant a (Å), bulk modulus B (GPa), total and orbital magnetic moment M and M_ℓ (μ_B), fundamental band gap Δ_{fund} (eV), and optical band gap Δ_{opt} (eV) of AFII phase of FeO.

	a	B	M (M_ℓ)	Δ_{fund}	Δ_{opt}
LDA	4.18	230	3.44 (0.09)	0.0	0.0
PBE	4.30	183	3.49 (0.08)	0.0	0.0
LDA+ U	4.28	199	4.23 (0.63)	1.7	2.2
B3PW91	4.35	172	4.15 (0.61)	1.3	1.8
B3LYP ^a	4.365	191		3.70	
PBE0	4.40	155	4.30 (0.75)	1.2	1.6
Fock-0.35	4.31	195	4.27 (0.68)	2.1	2.4
Fock-0.5	4.34	189	4.32 (0.68)	2.2	2.7
Expt.	4.334 ^b	150–180 ^c	3.32 ^d , 4.2 ^e	2.4 ^f	0.5 ^g , 2.4 ^h

^aReference 55.

^bReference 54.

^cSee Ref. 56 and references therein.

^dReference 57.

^eReference 58.

^fReference 51 (cited in Ref. 62).

^gAssigned to Fe 3d/O 2sp → Fe 4s transitions (Ref. 63).

^hAssigned to Fe 3d/O 2sp → Fe 3d transitions (Ref. 63).

separated parts, thus opening a band gap. PBE0 gives a position of the d peaks very similar to the one obtained with LDA+ U ($U_{\text{eff}}=5.91$ eV). The analysis of the peaks below the Fermi energy shows that the first narrow peak is mainly of Fe 3d character for LDA+ U , B3PW91, and PBE0 functionals, whereas for Fock-0.35 and Fock-0.5 functionals, it merges with lower peaks with a mixed Fe 3d/O 2p character. Experimentally, the top of the valence band was shown to be of mixed Mott-Hubbard/charge-transfer character⁶¹ or Mott-Hubbard character.⁵¹ Generally, a direct comparison between experimental and calculated fundamental band gaps should be done with care. In the case of FeO, such a comparison is particularly difficult due to the unclear experimental situation. Our calculated indirect fundamental band gaps seem to underestimate the experimental band gap of 2.4 eV reported in Ref. 51 (cited in Ref. 62), but considering the experimental XPS/BIS curve of Ref. 50 (shown in Fig. 2) an overestimation of the band gap could be also possible when comparing the position of the peaks just below and above the Fermi energy. The weak optical absorption between 0.5 and 2.0 eV reported in Ref. 63 could also indicate that our calculated fundamental band gaps are too large.

The observed differences in the DOSs are illustrated in Fig. 3 by showing the band structures of the PBE0 and Fock-0.5 hybrid functionals [the rhombohedral Brillouin zone is shown in Fig. 3(a) of Ref. 64]. With PBE0 we see just below the Fermi energy a band of Fe 3d character (corresponding to the sharp peak in the PBE0 DOS) which is well separated from the other lower-lying bands. For Fock-0.5, however, due to the large amount of HF exchange (50%), this Fe 3d band lies lower and mixes with the other bands, causing a band gap of mixed Mott-Hubbard/charge-transfer character.

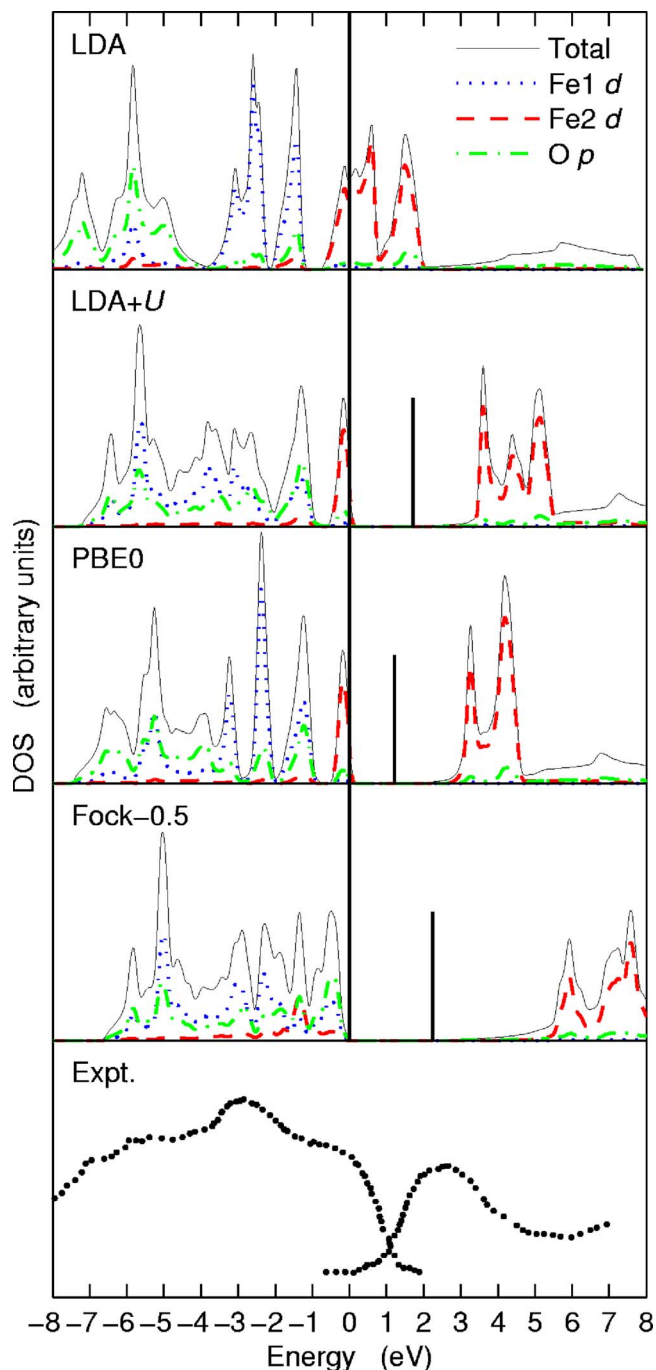


FIG. 2. (Color online) Same as Fig. 1 for FeO. The lowest panel shows the curve obtained from XPS/BIS measurements (Ref. 50).

C. CoO

From Table III we can see that again LDA largely underestimates the lattice constant a by ~ 0.15 Å with respect to the experimental value of 4.254 Å.⁶⁵ PBE is one of the best functionals for the lattice constant with 4.24 Å, while LDA+ U , with an underestimation of 0.05 Å, cannot completely repair the weakness of LDA. Fock-0.35 and Fock-0.5 yield the very good values of 4.24 and 4.27 Å, respectively, which means less than 0.02 Å of difference with respect to the experimental value. Comparing now our B3PW91 results with

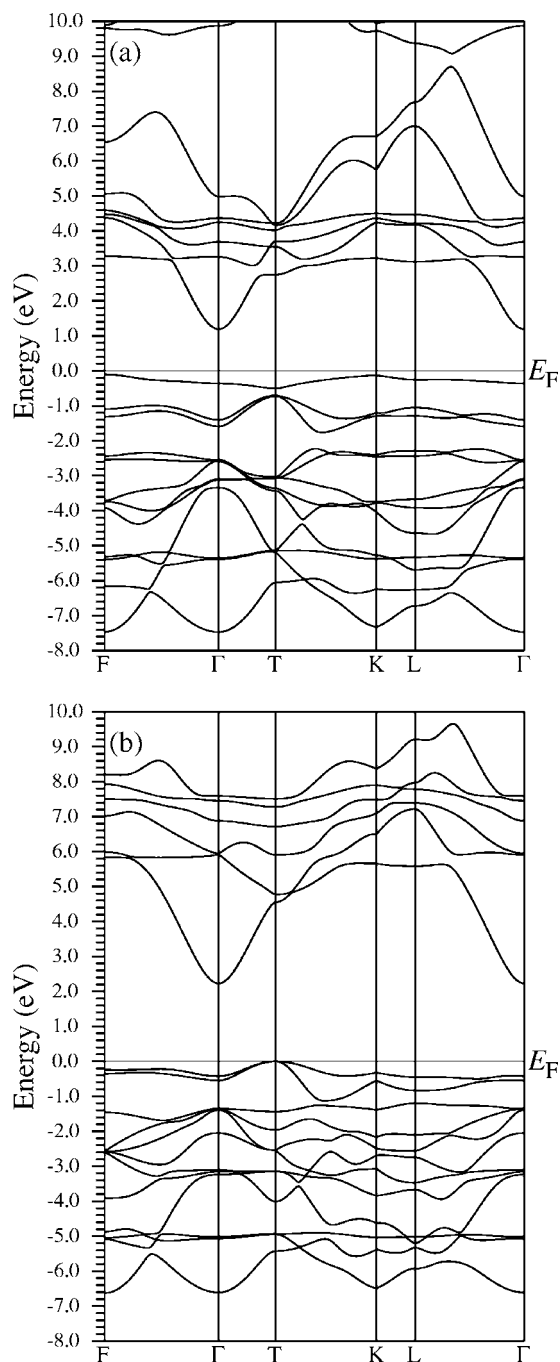


FIG. 3. PBE0 (a) and Fock-0.5 (b) band structures of AFII phase of FeO. The rhombohedral Brillouin zone is shown in Fig. 3(a) of Ref. 64.

the B3LYP (applied to all electrons) results of Bredow and Gerson¹⁰ we can see a nearly perfect agreement in the lattice constants between the two schemes (4.28 Å for B3PW91 vs 4.29 Å for B3LYP). For the bulk modulus B , the B3PW91 value (184 GPa) is the closest one to the experimental value [180 GPa (Ref. 66)].

As in the previously discussed case of FeO, a large orbital magnetic moment M_ℓ is expected for CoO. Solovyev *et al.*⁶⁷ and Shishidou and Jo⁶⁸ calculated for M_ℓ a value of about $1\mu_B$ with LDA+ U and Hartree-Fock methods, respectively, while Svane and Gunnarsson⁶⁹ obtained $1.2\mu_B$ with the self-

TABLE III. Same as Table II for CoO.

	a	B	$M (M_\ell)$	Δ_{fund}	Δ_{opt}
LDA	4.11	250	2.53 (0.17)	0.0	0.0
PBE	4.24	173	2.60 (0.17)	0.0	0.0
LDA+ U	4.20	212	3.48 (0.79)	2.7	3.6
B3PW91	4.28	184	3.23 (0.59)	2.0	3.0
B3LYP ^a	4.29		2.69 ^b	3.5	
B3LYP ^c	4.317		2.69 ^b	3.63	
PBE0	4.32	167	4.14 (1.48)	2.1	2.5
Fock-0.35	4.24	206	4.36 (1.65)	2.3	2.8
Fock-0.5	4.27	199	4.87 (2.10)	2.3	2.5
Expt.	4.254 ^d	180 ^e	3.35 ^f , 3.8 ^g , 3.98 ^h	2.5 ⁱ	2.7 ^j

^aReference 10.

^cReference 66.

ⁱReference 73.

^bValue for M_s .

^fReference 70.

^jReference 74.

^cReference 43.

^gReference 71.

^dReference 65.

^hReference 72.

interaction-corrected-LDA formalism. The results of our calculations show that the value of the orbital magnetic moment depends strongly on the used functional: LDA+ U and B3PW91 yield values well below $1\mu_B$, while PBE0, Fock-0.35, and Fock-0.5 values are well above $1\mu_B$. These different values of M_ℓ are the consequence of the fact that the considered orbital-dependent potentials do not lead to the same ground state (for each functional the presented results correspond to the state having the lowest total energy among the different ones we found), a characteristic which was not observed for FeO. For the total magnetic moment M only the LDA+ U value is situated within the range of the experimental values [$3.35\text{--}3.98\mu_B$ (Refs. 70–72)]. B3PW91 and PBE0 give values which are slightly underestimated and overestimated, respectively, while Fock-0.35 and Fock-0.5 hybrid functionals clearly overestimate the total magnetic moment. Note that the spin magnetic moment of $2.64\mu_B$ obtained with B3PW91 is very close to $2.69\mu_B$ which was calculated with the conventional B3LYP functional.^{10,43}

From the DOSs of CoO shown in Fig. 4, we can see that LDA+ U and hybrid functionals give a system of mixed Mott-Hubbard/charge-transfer character, in agreement with the experimental study of van Elp *et al.*⁷³ From XPS/BIS measurement, van Elp *et al.*⁷³ determined a band gap of about 2.5 eV, a value which falls within the range of the values for the fundamental indirect band gaps Δ_{fund} obtained with LDA+ U and hybrid functionals (2.0–2.7 eV). The comparison of the theoretical DOSs with the XPS/BIS curve⁷³ shows that LDA+ U , PBE0, and Fock-0.35 functionals give positions of the main peaks around the band gap which correspond roughly to the positions of the peaks of the XPS/BIS curve. Using 50% of HF exchange (Fock-0.5) pushes the unoccupied d peaks too high in energy. Finally, for the optical band gap Δ_{opt} , the experimentally determined value of 2.7 eV (Ref. 74) is well reproduced by the hybrid functionals which give values situated between 2.5 and 3.0 eV. LDA+ U , with $\Delta_{\text{opt}}=3.6$ eV yields a value which is about 1 eV too large.

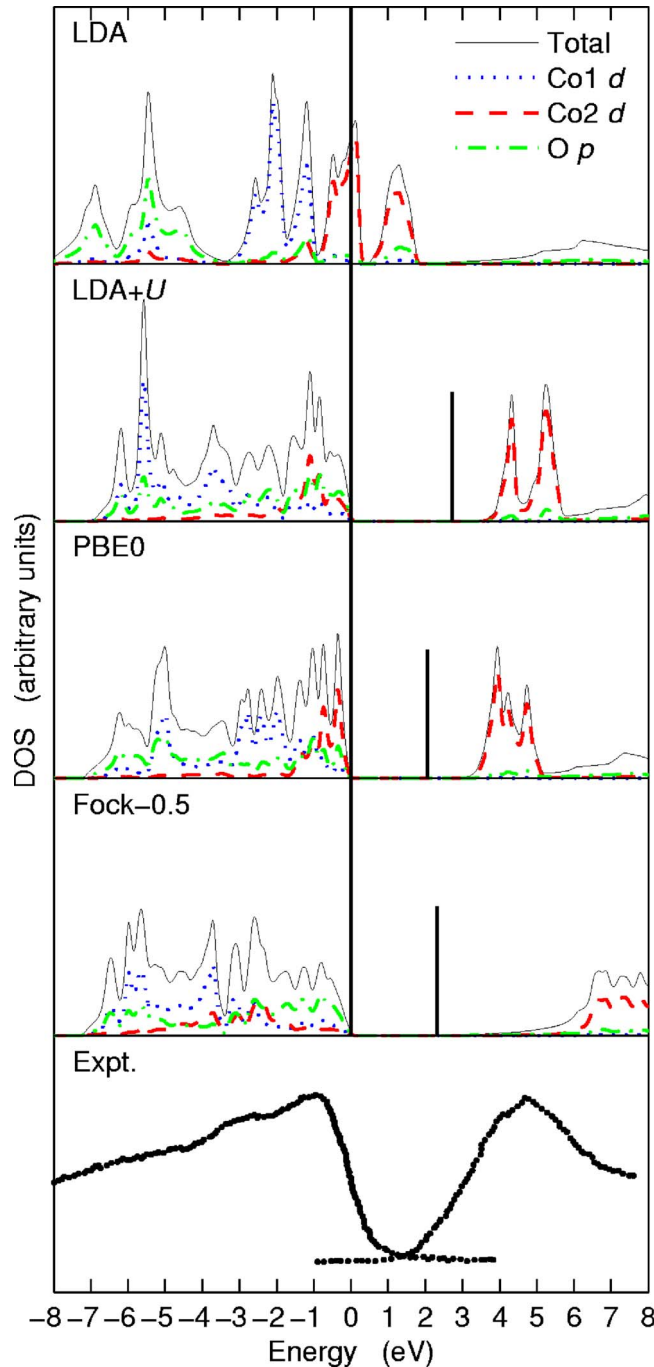


FIG. 4. (Color online) Same as Fig. 1 for CoO. The lowest panel shows the curve obtained from XPS/BIS measurements (Ref. 73).

D. NiO

For NiO, Table IV shows that Fock-0.35 and Fock-0.5 are the best functionals for the lattice constant with a difference of less than 0.02 Å with respect to the experimental value of 4.171 Å.⁷⁵ Moreira *et al.*³¹ obtained 4.14, 4.15, and 4.23 Å for the lattice constant with Fock-0.35, Fock-0.5, and B3LYP functionals, respectively, while our implementation of hybrid functionals gives 4.15, 4.18, and 4.21 Å with the same functionals (B3PW91 instead of B3LYP). Concerning the bulk modulus, PBE, B3PW91, and PBE0 functionals seem to be

TABLE IV. Same as Table I for NiO.

	a	B	M_s	Δ_{fund}	Δ_{opt}
LDA	4.07	257	1.21	0.4	0.6
PBE	4.20	197	1.38	0.9	1.1
LDA+ U	4.12	234	1.72	3.2	4.0
B3PW91	4.21	203	1.70	2.8	3.4
B3LYP ^a	4.227		1.67	4.1	
B3LYP ^b	4.218–4.225	198–209	1.67	4.2	
PBE0	4.24	187	1.73	2.8	3.4
Fock-0.35	4.15	227	1.78	2.9	3.5
Fock-0.35 ^a	4.144		1.75	6.2	
Fock-0.5	4.18	218	1.84	3.0	3.5
Fock-0.5 ^a	4.152		1.81	8.4	
Expt.	4.171 ^c	166–208 ^d	1.64 ^e , 1.90 ^f	4.0 ^g , 4.3 ^h	3.1 ⁱ

^aReference 31.

^dReference 76.

^gReference 81.

^bReference 77.

^eReference 78.

^hReference 82.

^cReference 75.

^fReference 47.

ⁱReference 74.

the best performing with values within the experimental range of 166–208 GPa.⁷⁶ Our calculated B3PW91 value of $B=203$ GPa agrees well with the range 198–209 GPa of B3LYP values of Feng and Harrison.⁷⁷

LDA+ U and all hybrid functionals give values of the spin magnetic moment M_s within the experimental range [1.64 – $1.90\mu_B$ (Refs. 47 and 78)]. The values calculated by Moreira *et al.*³¹ for M_s are 1.75, 1.81, and $1.67\mu_B$, for Fock-0.35, Fock-0.5, and B3LYP functionals, respectively, while our corresponding values are 1.78, 1.84, and $1.70\mu_B$.

The DOSs of NiO, shown in Fig. 5, reveal that using LDA+ U or hybrid functionals give a valence band of mixed Ni 3d/O 2p character. As expected, the band gap obtained by the Fock-0.5 hybrid functional is the one showing the largest fraction of charge-transfer character, which dominates in this case. Experimentally, NiO has been described as a charge-transfer⁷⁹ insulator or more recently, using site-specific soft x-ray emission and/or absorption and site-specific XPS spectroscopies, as a mixed Mott-Hubbard/charge-transfer⁸⁰ insulator. Again, as for FeO and CoO, the PBE0 functional gives a position of the unoccupied Ni 3d DOS which is very close to the LDA+ U ($U_{\text{eff}}=7.05$ eV) one. The calculated fundamental band gap Δ_{fund} obtained with LDA+ U or hybrid functionals, and indirect in all cases, is ~ 3 eV which is ~ 1 eV below the experimental values of 4.0 (Ref. 81) and 4.3 eV.⁸² Nevertheless, the comparison of the calculated DOSs with XPS/BIS spectra obtained from Refs. 50 and 82 shows that the position of the peaks below and above the band gap are well reproduced by LDA+ U and PBE0 functionals. The hybrid functionals, but not LDA+ U , well reproduce the experimental optical band gap⁷⁴ (3.1 eV) with an overestimation of only ~ 0.4 eV.

IV. SUMMARY AND CONCLUSION

An approximate but computationally efficient hybrid method has been applied to the transition-metal monoxides,

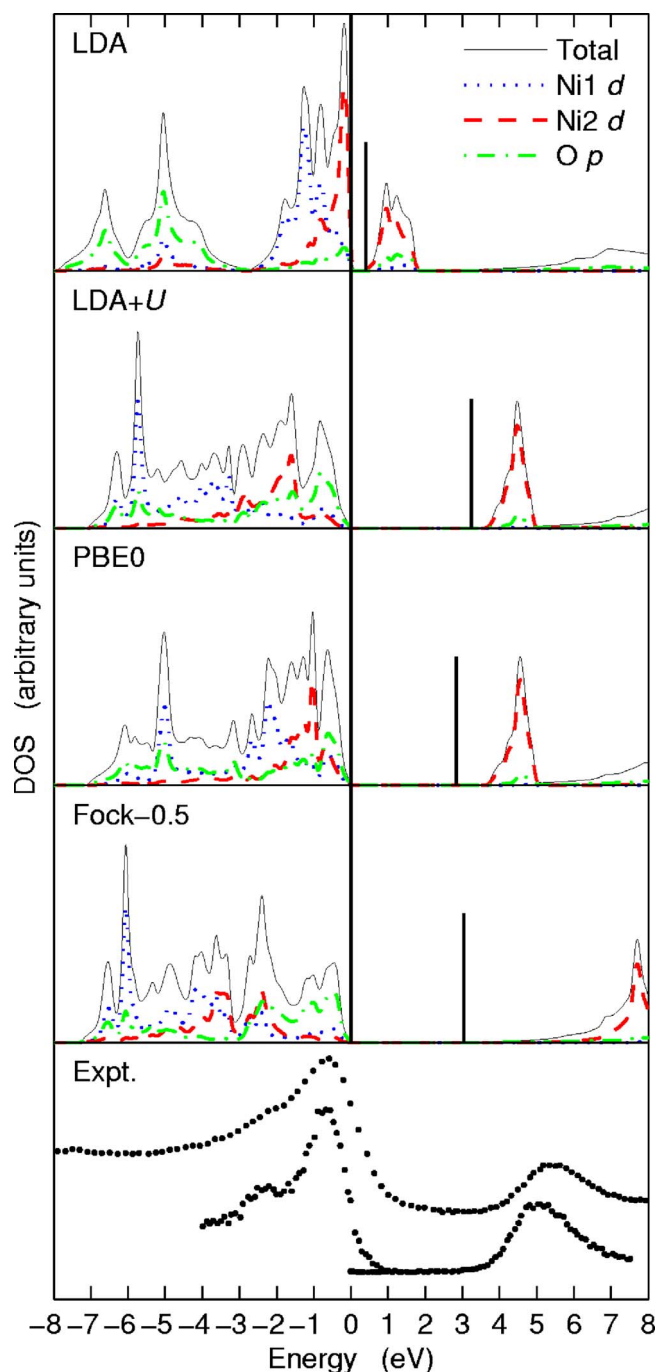


FIG. 5. (Color online) Same as Fig. 1 for NiO. The lowest panel shows curves obtained from XPS/BIS measurements by Sawatzky and Allen (Ref. 82) (lower curve) and Zimmermann *et al.* (Ref. 50) (upper curve).

MnO, FeO, CoO, and NiO. This method, which is similar to the LDA+ U method, but without system-dependent parameters (the amount of HF exchange is an *a priori* fixed param-

eter), leads to an implementation that is computationally much simpler than the full implementation of HF equations conventionally used within hybrid methods. The presented scheme is particularly suited for systems having strongly correlated (localized) electrons (usually d or f electrons) which are not described well by conventional exchange-correlation energy functionals of the LDA and GGA forms. The present work has shown that applying hybrid functionals only inside the atomic sphere and to the $3d$ electrons of the transition metals can lead to very accurate results, describing correctly both the structural and electronic properties. In particular, Fock-0.35 and Fock-0.5 yield very accurate lattice constants (typically with a deviation of 0.01–0.02 Å), in better agreement with experiment than LDA, LDA+ U , and sometimes PBE. The bulk modulus is better described by the B3PW91 hybrid functional compared to other functionals. The electronic properties are also described fairly well. The hybrid functionals reproduce very well the trends of LDA+ U which was designed to significantly improve over LDA and GGA for systems containing strongly correlated electrons. The results with our scheme are also in good agreement with those obtained from the conventional application of hybrid functionals to all electrons, particularly for the lattice constant and the magnetic moment. For the fundamental band gap (our values are smaller) the differences come from the fact that in our scheme, the HF exchange is applied only to the $3d$ electrons. In some cases this makes our band gap in better agreement with experiment.

Nevertheless, for the itinerant magnetic systems like Fe, Co, and Ni, for which LDA and GGA work quite well for the structural and electronic properties, we expect the hybrid functionals to give, e.g., too large magnetic moments because of the HF exchange, as already reported in Refs. 15 and 83 using other implementations of the HF method.

It is quite fair to say that this hybrid scheme represents a very efficient alternative to LDA+ U . In the case of large systems, this hybrid scheme can become very useful as the treatment of the full HF exchange is computationally very demanding. In order to confirm this conclusion, an application of this method to f electrons in rare-earth compounds is desirable and thus such work is in progress.

ACKNOWLEDGMENTS

This work was supported by project A1010214 of the Grant Agency of the ASCR and the AURORA project SFB011 of the Austrian Science Foundation. One of the authors (F.T.) is grateful for support from the Swiss National Science Foundation (Grant No. PBGE2-108846) and acknowledges support from the European Community's Human Potential Program under Contract No. HPRN-CT-2002-00293, SCOOTMO, during his stay at the Institute of Physics, ASCR, Prague.

- ¹W. Kohn and L. J. Sham, Phys. Rev. **140**, A1133 (1965).
- ²P. Hohenberg and W. Kohn, Phys. Rev. **136**, B864 (1964).
- ³A. D. Becke, J. Chem. Phys. **98**, 1372 (1993).
- ⁴A. D. Becke, J. Chem. Phys. **98**, 5648 (1993).
- ⁵V. N. Staroverov, G. E. Scuseria, J. Tao, and J. P. Perdew, J. Chem. Phys. **119**, 12129 (2003); **121**, 11507 (2004).
- ⁶R. N. Euwema, D. L. Wilhite, and G. T. Surratt, Phys. Rev. B **7**, 818 (1973).
- ⁷A. Svane, Phys. Rev. B **35**, 5496 (1987).
- ⁸C. Pisani, R. Dovesi, and C. Roetti, in *Hartree-Fock ab initio Treatment of Crystalline Systems*, Vol. 48 of Lecture Notes in Chemistry, edited by G. Berthier, M. J. S. Dewar, H. Fischer, K. Fukui, G. G. Hall, J. Hinze, H. H. Jaffé, J. Jortner, W. Kutzelnigg, K. Ruedenberg, and J. Tomasi (Springer-Verlag, Heidelberg, 1988).
- ⁹S. Massidda, M. Posternak, and A. Baldereschi, Phys. Rev. B **48**, 5058 (1993).
- ¹⁰T. Bredow and A. R. Gerson, Phys. Rev. B **61**, 5194 (2000).
- ¹¹J. Muscat, A. Wander, and N. M. Harrison, Chem. Phys. Lett. **342**, 397 (2001).
- ¹²R. Dovesi, R. Orlando, C. Roetti, C. Pisani, and V. R. Saunders, Phys. Status Solidi B **217**, 63 (2000).
- ¹³A. V. Nikolaev and P. N. Dyachkov, Int. J. Quantum Chem. **89**, 57 (2002); **93**, 375 (2003).
- ¹⁴J. Heyd, G. E. Scuseria, and M. Ernzerhof, J. Chem. Phys. **118**, 8207 (2003).
- ¹⁵I. Schnell, G. Czycholl, and R. C. Albers, Phys. Rev. B **68**, 245102 (2003).
- ¹⁶J. Paier, R. Hirschl, M. Marsman, and G. Kresse, J. Chem. Phys. **122**, 234102 (2005).
- ¹⁷A. Sorouri, W. M. C. Foulkes, and N. D. M. Hine, J. Chem. Phys. **124**, 064105 (2006).
- ¹⁸P. Novák, J. Kuneš, L. Chaput, and W. E. Pickett, Phys. Status Solidi B **243**, 563 (2006).
- ¹⁹M. Städele, J. A. Majewski, P. Vogl, and A. Görling, Phys. Rev. Lett. **79**, 2089 (1997).
- ²⁰R. J. Magyar, A. Fleszar, and E. K. U. Gross, Phys. Rev. B **69**, 045111 (2004).
- ²¹S. Sharma, J. K. Dewhurst, and C. Ambrosch-Draxl, Phys. Rev. Lett. **95**, 136402 (2005).
- ²²F. Corà, M. Alfredsson, G. Mallia, D. S. Middlemiss, W. C. Mackrodt, R. Dovesi, and R. Orlando, Struct. Bonding (Berlin) **113**, 171 (2004).
- ²³M. Ernzerhof and G. E. Scuseria, J. Chem. Phys. **110**, 5029 (1999).
- ²⁴C. Adamo and V. Barone, J. Chem. Phys. **110**, 6158 (1999).
- ²⁵J. P. Perdew, K. Burke, and M. Ernzerhof, Phys. Rev. Lett. **77**, 3865 (1996); **78**, 1396(E) (1997).
- ²⁶J. P. Perdew, M. Ernzerhof, and K. Burke, J. Chem. Phys. **105**, 9982 (1996).
- ²⁷P. A. M. Dirac, Proc. Cambridge Philos. Soc. **26**, 376 (1930).
- ²⁸J. P. Perdew and Y. Wang, Phys. Rev. B **45**, 13244 (1992).
- ²⁹A. D. Becke, Phys. Rev. A **38**, 3098 (1988).
- ³⁰J. P. Perdew, J. A. Chevary, S. H. Vosko, K. A. Jackson, M. R. Pederson, D. J. Singh, and C. Fiolhais, Phys. Rev. B **46**, 6671 (1992); **48**, 4978(E) (1993).
- ³¹I. de P. R. Moreira, F. Illas, and R. L. Martin, Phys. Rev. B **65**, 155102 (2002).
- ³²S. H. Vosko, L. Wilk, and M. Nusair, Can. J. Phys. **58**, 1200 (1980).
- ³³P. Blaha, K. Schwarz, G. K. H. Madsen, D. Kvasnicka, and J. Luitz, in *WIEN2K, An Augmented Plane Wave and Local Orbitals Program for Calculating Crystal Properties*, edited by K. Schwarz (Vienna University of Technology, Austria, 2001).
- ³⁴V. I. Anisimov, J. Zaanen, and O. K. Andersen, Phys. Rev. B **44**, 943 (1991).
- ³⁵A. I. Liechtenstein, V. I. Anisimov, and J. Zaanen, Phys. Rev. B **52**, R5467 (1995).
- ³⁶V. I. Anisimov, F. Aryasetiawan, and A. I. Liechtenstein, J. Phys.: Condens. Matter **9**, 767 (1997).
- ³⁷A. B. Shick, A. I. Liechtenstein, and W. E. Pickett, Phys. Rev. B **60**, 10763 (1999).
- ³⁸K. Terakura, T. Oguchi, A. R. Williams, and J. Kübler, Phys. Rev. B **30**, 4734 (1984).
- ³⁹P. Dufek, P. Blaha, V. Sliwko, and K. Schwarz, Phys. Rev. B **49**, 10170 (1994).
- ⁴⁰M. Cococcioni and S. de Gironcoli, Phys. Rev. B **71**, 035105 (2005).
- ⁴¹R. W. G. Wyckoff, *Crystal Structures* (Interscience, New York, 1964).
- ⁴²C. Franchini, V. Bayer, R. Podloucky, J. Paier, and G. Kresse, Phys. Rev. B **72**, 045132 (2005).
- ⁴³X. Feng, Phys. Rev. B **69**, 155107 (2004).
- ⁴⁴P. J. Stephens, F. J. Devlin, C. F. Chabalowski, and M. J. Frisch, J. Phys. Chem. **98**, 11623 (1994).
- ⁴⁵Y. Noguchi, K. Kusaba, K. Fukuoka, and Y. Syono, Geophys. Res. Lett. **23**, 1469 (1996).
- ⁴⁶R. Jeanloz and A. Rudy, J. Geophys. Res. **92**, 11433 (1987).
- ⁴⁷A. K. Cheetham and D. A. O. Hope, Phys. Rev. B **27**, 6964 (1983).
- ⁴⁸B. E. F. Fender, A. J. Jacobson, and F. A. Wedgwood, J. Chem. Phys. **48**, 990 (1968).
- ⁴⁹J. van Elp, R. H. Potze, H. Eskes, R. Berger, and G. A. Sawatzky, Phys. Rev. B **44**, 1530 (1991).
- ⁵⁰R. Zimmermann, P. Steiner, R. Claessen, F. Reinert, S. Hüfner, P. Blaha, and P. Dufek, J. Phys.: Condens. Matter **11**, 1657 (1999).
- ⁵¹J. van Elp, Ph.D. thesis, University of Groningen, 1991.
- ⁵²A. Fujimori, N. Kimizuka, T. Akahane, T. Chiba, S. Kimura, F. Minami, K. Satoro, M. Taniguchi, S. Ogawa, and S. Suga, Phys. Rev. B **42**, 7580 (1990).
- ⁵³D. R. Huffman, R. L. Wild, and M. Shinmei, J. Chem. Phys. **50**, 4092 (1969).
- ⁵⁴C. A. McCammon and L.-G. Liu, Phys. Chem. Miner. **10**, 106 (1984).
- ⁵⁵M. Alfredsson, G. D. Price, C. R. A. Catlow, S. C. Parker, R. Orlando, and J. P. Brodholt, Phys. Rev. B **70**, 165111 (2004).
- ⁵⁶S. D. Jacobsen, H.-J. Reichmann, H. A. Spetzler, S. J. Mackwell, J. R. Smyth, R. J. Angel, and C. A. McCammon, J. Geophys. Res. **107**, 2037 (2002).
- ⁵⁷W. L. Roth, Phys. Rev. **110**, 1333 (1958).
- ⁵⁸P. D. Battle and A. K. Cheetham, J. Phys. C **12**, 337 (1979).
- ⁵⁹I. V. Solovyev, A. I. Liechtenstein, and K. Terakura, J. Magn. Magn. Mater. **185**, 118 (1998).
- ⁶⁰Z. Fang, I. V. Solovyev, H. Sawada, and K. Terakura, Phys. Rev. B **59**, 762 (1999).
- ⁶¹P. S. Bagus, C. R. Brundle, T. J. Chuang, and K. Wandelt, Phys. Rev. Lett. **39**, 1229 (1977).
- ⁶²F. Parmigiani and L. Sangaletti, J. Electron Spectrosc. Relat. Phenom. **98-99**, 287 (1999).
- ⁶³I. Balberg and H. L. Pinch, J. Magn. Magn. Mater. **7**, 12 (1978).

- ⁶⁴J. E. Pask, D. J. Singh, I. I. Mazin, C. S. Hellberg, and J. Kortus, *Phys. Rev. B* **64**, 024403 (2001).
- ⁶⁵M. J. Carey, F. E. Spada, A. E. Berkowitz, W. Cao, and G. Thomas, *J. Mater. Res.* **6**, 2680 (1991).
- ⁶⁶Q. Guo, H.-K. Mao, J. Hu, J. Shu, and R. J. Hemley, *J. Phys.: Condens. Matter* **14**, 11369 (2002).
- ⁶⁷I. V. Solovyev, A. I. Liechtenstein, and K. Terakura, *Phys. Rev. Lett.* **80**, 5758 (1998).
- ⁶⁸T. Shishidou and T. Jo, *J. Phys. Soc. Jpn.* **67**, 2637 (1998).
- ⁶⁹A. Svane and O. Gunnarsson, *Phys. Rev. Lett.* **65**, 1148 (1990).
- ⁷⁰D. C. Khan and R. A. Erickson, *Phys. Rev. B* **1**, 2243 (1970).
- ⁷¹D. Herrmann-Ronzaud, P. Burlet, and J. Rossat-Mignod, *J. Phys. C* **11**, 2123 (1978).
- ⁷²W. Jauch, M. Reehuis, H. J. Bleif, F. Kubanek, and P. Pattison, *Phys. Rev. B* **64**, 052102 (2001).
- ⁷³J. van Elp, J. L. Wieland, H. Eskes, P. Kuiper, G. A. Sawatzky, F. M. F. de Groot, and T. S. Turner, *Phys. Rev. B* **44**, 6090 (1991).
- ⁷⁴R. J. Powell and W. E. Spicer, *Phys. Rev. B* **2**, 2182 (1970).
- ⁷⁵L. C. Bartel and B. Morosin, *Phys. Rev. B* **3**, 1039 (1971).
- ⁷⁶E. Huang, K. Jy, and S.-C. Yu, *J. Geophys. Soc. China* **37**, 7 (1994).
- ⁷⁷X.-B. Feng and N. M. Harrison, *Phys. Rev. B* **69**, 035114 (2004).
- ⁷⁸H. A. Alperin, *J. Phys. Soc. Jpn.* **17**, Suppl. B-III, 12 (1962).
- ⁷⁹J. van Elp, H. Eskes, P. Kuiper, and G. A. Sawatzky, *Phys. Rev. B* **45**, 1612 (1992).
- ⁸⁰T. M. Schuler, D. L. Ederer, S. Itza-Ortiz, G. T. Woods, T. A. Callcott, and J. C. Woicik, *Phys. Rev. B* **71**, 115113 (2005).
- ⁸¹S. Hüfner, J. Osterwalder, T. Riesterer, and F. Hulliger, *Solid State Commun.* **52**, 793 (1984).
- ⁸²G. A. Sawatzky and J. W. Allen, *Phys. Rev. Lett.* **53**, 2339 (1984).
- ⁸³J. Paier, M. Marsman, K. Hummer, G. Kresse, I. C. Gerber, and J. G. Ángyán, *J. Chem. Phys.* **124**, 154709 (2006).